EGU2020-14540

Impact of elastic material properties and discontinuities on the stress orientation

Karsten Reiter (reiter@geo.tu-darmstadt.de)
TU Darmstadt, Institute of Applied Geosciences, Schnittspahnstraße 9, 64287 Darmstadt, Germany

TECHNISCHE UNIVERSITÄT DARMSTADT

Objective

The in-situ stress state in the upper crust is an important issue for diverse economic purposes and scientific questions as well. Several methods have been established in the last decades to estimate the present-day orientation of the maximum compressive horizontal stress (S_{Hmax}) in the crust. It has been assumed, that the S_{Hmax} orientation on a regional scale is governed by the same forces that drive plate motion too. The S_{Hmax} orientation data, compiled by the World Stress Map (WSM) project, confirmed that for many regions in the world. Due to the increasing amount of data, it is now possible to identify several areas in the world, where stress orientation deviates from the expected orientation due to plate boundary forces (first order stress sources), or the plate wide pattern. In some of this regions a gradual rotation of the S_{Hmax} orientation is observed.

Stress rotations

Several second and third order stress sources have been identified which may explain stress rotation in the upper crust. For example, lateral heterogeneities in the crust, such as density, petrophysical or petrothermal properties and discontinuities, like faults are identified. Apparently, there are just a few studies, that deal with the potential extend of stress rotation as a function of second and third order stress sources. For that reason, generic geomechanical numerical models have been developed, consisting of up to five different units oriented at an angle of 60 degrees to the direction of contraction. These units have variable elastic material properties, such as Young's modulus, Poisson ratio and density. In addition, an identical model geometry allows the units to be separated by contact surfaces that allow them so slide along the faults, depending on a selected coefficient of friction.

Material properties and discontinuities

The model results indicate, that a density contrast (Fig. 4) or the variation of the Poisson's ratio (Fig. 5) alone sparsely rotates the horizontal stress orientation. Conversely, a contrast of the Young's modulus (Fig. 6) allows significant stress rotations. Not only areas in the vicinity of the material transition are affected by the stress rotation, but the entire blocks. Low friction discontinuities do not change the stress pattern when viewed over a wide area in homogeneous models (Fig. 7). This also applies to models with alternating stiff and soft blocks - the stress orientation is determined solely by the boundary conditions, not the material transitions (Fig. 8). This indicates that material contrasts are capable of producing significant stress rotation for larger areas in the crust. Active faults that separates such material contrasts have the opposite effect, they compensate for stress rotations.

Model geometry and material properties

Name	Young's Modulus [GPa]	Poissons ratio [-]	Density [kg m^{-3}]
Basic	50	0.25	2700
Hard	**100**	0.25	2700
Soft	**10**	0.25	2700
Low Density	50	0.25	**2200**
High Density	50	0.25	**3200**
Low Poisson	50	**0.15**	2700
High Poissons	50	**0.35**	2700

Table 1. Used elastic material properties and density. Background colours indicate the material, which are used in the model visualisations. Bold numbers have different properties then the basic material.

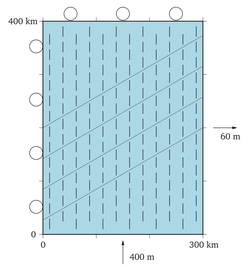

Figure 1. Principle geometry of the models and used boundary conditions. The model has an extend of 400 x 300 x 30 km and is shortened by 400 m in North-South direction and pulled in East-West direction by 60 m, to to generate appropriate stress magnitudes (see Fig. 2 and Fig. 3). The stress orientation is visualized in a depth of 1000 m; S_{Hmax} is parallel to the bars.

Stress magnitudes and stress ratio in the basic model

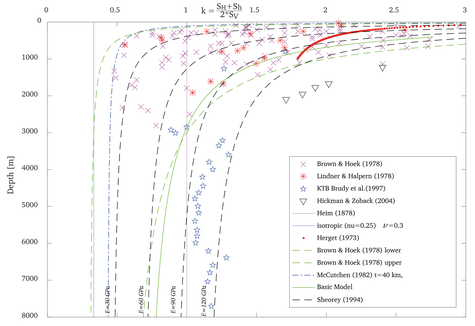

Figure 3. Stress ratio k versus depth of the basic model combined with several data and defined stress ratios from the literature (Brown & Hoeck 1978, Lindner & Halpern 1978, Brudy et al. 1997, Hickman & Zoback 2004, Heim 1878, Herget 1973, Mc Cutchen 1982, Sheorey 1994).

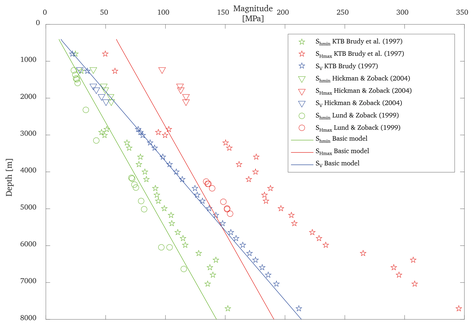

Figure 2. Stress magnitudes versus depth are shown from the center of the basic model using boundary conditions, illustrated in Fig. 1. Due to applied initial stress conditions, the stress regime switches from thrust faulting at about 400 m depth to strike slip faulting, and in a depth of about 5500m to normal faulting. Published stress magnitude data are shown for comparison (Brudy et al. 1997, Hickman & Zoback 2004, Lund & Zoback 1999). Note: S_{Hmax} data are not measured, they are calculated based on S_{hmin} magnitudes and several assumptions.

References:
Brown, E. T., & Hoek, E. (1978). Trends in relationships between measured in-situ stresses and depth. International Journal of Rock Mechanics and Mining Sciences & Geomechanics Abstracts, 15(4), 211–215, doi: 10.1016/0148-9062(78)91227-5.
Brudy, M., Zoback, M. D., Fuchs, K., Rummel, F., & Baumgärtner, J. (1997). Estimation of the complete stress tensor to 8 km depth in the KTB scientific drill holes: Implications for crustal strength. Journal of Geophysical Research, 102(B8), 18453, doi: 10.1029/96JB02942.
Heim, A. (1878). Untersuchungen über den Mechanismus der Gebirgsbildung im Anschluss an die geologische Monographie der Tödi-Windgällen-Gruppe. Basel: Benno Schwabe Verlagsbuchhandlung.
Herget, G. (1973). Variation of rock stresses with depth at a Canadian iron mine. International Journal of Rock Mechanics and Mining Sciences & Geomechanics Abstracts, 10(1), 37–51, doi: 10.1016/0148-9062(73)90058-2.
Hickman, S., & Zoback, M. D. (2004). Stress orientations and magnitudes in the SAFOD pilot hole. Geophysical Research Letters, 31(15), L15S12, doi: 10.1029/2004GL020043.
Lindner, E. N., & Halpern, J. A. (1978). In-situ stress in North America: A compilation. International Journal of Rock Mechanics and Mining Sciences & Geomechanics Abstracts, 15(4), 183–203, doi: 10.1016/0148-9062(78)91225-1.
Lund, B., & Zoback, M. . (1999). Orientation and magnitude of in situ stress to 6.5 km depth in the Baltic Shield. International Journal of Rock Mechanics and Mining Sciences, 36(2), 169–190, doi: 10.1016/S0148-9062(98)00185-1.
McCutchen, W. R. R. (1982). Some elements of a theory for In-situ stress. International Journal of Rock Mechanics and Mining Sciences & Geomechanics Abstracts, 19(4), 201–203.
Sheorey, P. R. R. (1994). A theory for In Situ stresses in isotropic and transverseley isotropic rock. International Journal of Rock Mechanics and Mining Sciences & Geomechanics Abstracts, 31(1), 23–34, doi: 10.1016/0148-9062(94)92312-4.

Density variation

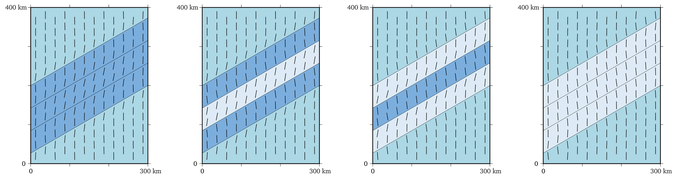

Figure 4. Effect of stress rotation due to density variation. Colours indicate different densities (see Table 1.) Orientation of S_{Hmax} is indicated by black bars.

Variation of Poisson's ratio

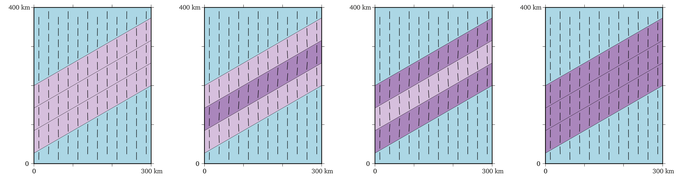

Figure 5. Effect of stress rotation due to variation of Poisson's ratio. Colours indicate different Poisson's ratios (see Table 1.) Orientation of S_{Hmax} is indicated by black bars.

Variation of Young's modulus

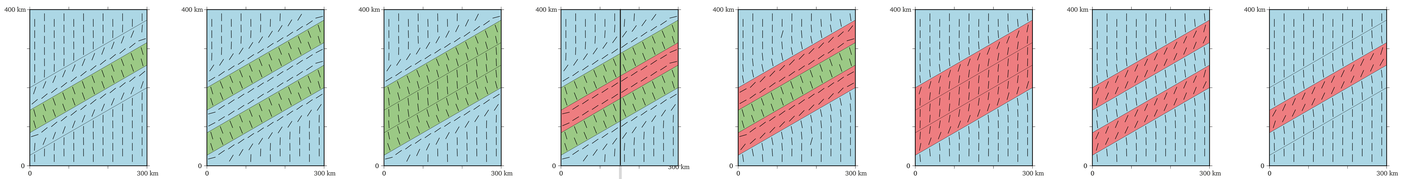

Figure 6. Effect of stress rotation due to variation of Young's modulus. Colours indicate different Young's modulus (see Table 1.) Orientation of S_{Hmax} is indicated by black bars. The black vertical line indicates the location of the profile in Fig. 9.

Variation of friction coefficient along the discontinuities

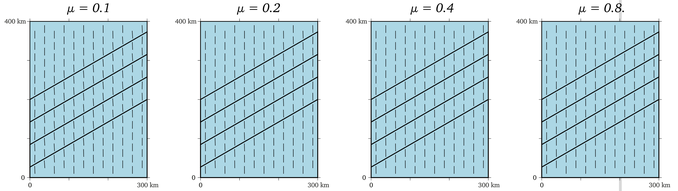

Figure 7. Effect of stress rotation due to different friction coefficients along four discontinuities. Orientation of S_{Hmax} is indicated by black bars.

Variation of Young's modulus combined with low friction coefficient

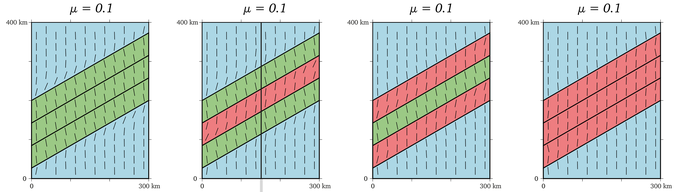

Figure 8. Effect of stress rotation due to low friction along the faults and variation of Young's modulus. Colours indicate different Young's modulus (see Table 1.) Orientation of S_{Hmax} is indicated by black bars. The black vertical line indicates the location of the profile in Fig. 10.

Stress orientation profiles

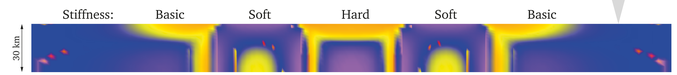

Figure 9. Orientation of S_{Hmax} is colour-coded, see Legend. S_{Hmax} ist oriented around 40° in the stiffer units next to the softer units in the upper part. A similar orientation can be observed in the soft units in the deepest parts.

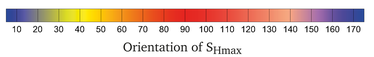

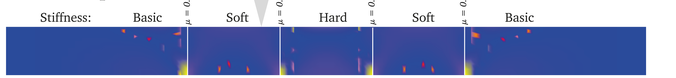

Figure 10. Orientation of S_{Hmax} is colour-coded, see Legend. In contrast to the similar model profile in Fig. 9, the discontinuities with a low friction coefficient counterbalances stress reorientation effects by stiffness contrasts.